This is a preview version of our white paper on LED and photodiode photonic devices

To get the full version, just send us an e-mail: **info@idonus.com**

WHITE PAPER

Broadband radiometric measurement of light-emitting diodes with a photodiode

The spectral characteristics of the light-emitting diode (LED) and the photodiode are well explained by quantum mechanics. Based on this knowledge, we will demonstrate how our multi-wavelength LED light source can be measured with a photodiode.

www.idonus.com
Written by C. Yamahata, idonus sàrl
Issued in December 2020

The spectral power distribution of a light-emitting diode (LED) has a distinctive asymmetrical gaussian shape. This is the macroscopic expression of finely tuned properties buried inside the semiconductor. In this white paper, we unveil why and how a photodiode can be used as a reliable radiometric instrument for the characterisation of broadband LEDs. The key idea is to use prior knowledge of the centroid wavelength λ_c of the emitted light and account for it to calculate the responsivity $\Re(\lambda_c)$ of the photodiode.

1. Introduction

Basic science is primarily a discipline based on observation. Many fundamental discoveries owe much to the quality of the underlying observations, *i.e.* the precise and accurate measurement of phenomena. A fascinating story that illustrates this is that of Kepler's laws describing the motion of the planets around the Sun. If Johannes Kepler succeeded to make his extraordinary discoveries, it is undeniably because he had extremely accurate data from Tycho Brahe, especially his meticulous observations of Mars recorded over a whole decade. Kepler, who had been Brahe's assistant, knew that these data were absolutely reliable, and definitely the most accurate at the time.

The discovery of quantum mechanics is also closely linked to the development of accurate instrumentation, particularly that used for the build and characterisation of blackbody radiation. Here, we are interested in the spectral characterisation of LEDs. In section 3, we will present the study of blackbody radiation and see that it is a very suitable entry point to tackle this subject. Our approach being made from a historical perspective, this will lead us to talk about the discovery of the photoconductive effect in section 4. Section 5 will be devoted to semiconductor properties and their use in photonic devices: the photodiode, whose responsivity model will be presented in section 6; the LED, whose characteristic electroluminescence spectrum will be explained in section 7. Finally, in section 8, with the help of the technical developments presented in previous sections, we will be able to develop the main idea of this document: namely, the use of the photodiode for radiometric measurement of broadband LEDs. Before that, we will first introduce in section 2 the fundamental constants that will be used throughout this paper.

2. The seven defining constants of the International System of units

As early as 1900, Max Planck suggested that the two constants k_B (now known as the Boltzmann constant)[1] and h (the Planck constant) which appear in his equation of radiation entropy, together with the speed of light in vacuum c and the gravitational constant G,[2] could be used as

> [fundamental constants] to define units for the length, mass, time and temperature, which are independent of special bodies or substances, keep their significance for all times and for all, including extra-terrestrial and non-human civilisations, and can therefore be called "natural units of measurement".
>
> — Max Planck [1], p. 121.
> *(quotation translated from the original German text)*

At that time, the centimetre–gram–second (CGS) system of units was the predominant system used for scientific purposes. The CGS was superseded by the metre–kilogram–second (MKS) system, which in turn was extended (MKSA, the A standing for ampere) and finally replaced by the International System of Units (SI), the modern form of the metric system. The SI was created in 1960 and has become the universal system of units and the standard measurement language for trade and science.

Since 1971, the SI consists of seven base units which are the **metre** (the unit of length with the symbol m), the **kilogram** (mass, kg), the **second** (time, s), the **ampere** (electric current, A), the **kelvin** (thermodynamic temperature, K), the **mole** (amount of substance, mol), and the **candela** (luminous intensity, cd). In 2019, the SI made a decisive step forward. From that date, the magnitudes of all SI units have been defined by declaring exact numerical values for seven defining constants (see Table 1). These defining constants are the speed of light in vacuum c (defining constant for the meter, $c \rightarrow$ m), the Planck constant h ($h \rightarrow$ kg), the hyperfine transition frequency of caesium $\Delta\nu_{Cs}$ ($\Delta\nu_{Cs} \rightarrow$ s), the elementary charge e ($e \rightarrow$ A), the Boltzmann constant k_B ($k_B \rightarrow$ K), the Avogadro constant N_A ($N_A \rightarrow$ mol), and the luminous efficacy K_{cd} ($K_{cd} \rightarrow$ cd). It is quite remarkable that three of these defining constants happen to be those that had been advised more than a century before by Planck.

[1] For the sake of consistency with the rest of the document, we have adapted several historical formulas using today's most commonly accepted symbols.

[2] Newtonian constant of gravitation, $G = 6.67408 \times 10^{-11}$ m^3.kg^{-1}.s^{-2} (2018 CODATA recommended value).

__Table 1:__ The seven defining constants of the International System of Units (SI).

Defining constant	Symbol	Numerical value	Unit
speed of light in vacuum	c	299 792 458	m.s^{-1}
Planck constant [a]	h	6.626 070 15 ×10^{-34}	J.s
hyperfine transition frequency of caesium-133 (^{133}Cs)	$\Delta\nu_{\mathrm{Cs}}$	9 192 631 770	s^{-1}
elementary charge [a]	e	1.602 176 634 ×10^{-19}	C
Boltzmann constant [a]	k_{B}	1.380 649 ×10^{-23}	J.K^{-1}
Avogadro constant [a]	N_{A}	6.022 140 76 ×10^{23}	mol^{-1}
luminous efficacy of 540 THz radiation [b]	K_{cd}	683	lm.W^{-1}

a) These numerical values have been fixed to their best estimates, as calculated from the 2017 CODATA special adjustment.
b) Using the relation $\lambda = c/\nu$ and considering a monochromatic radiation of frequency ν = 5.4 ×10^{14} Hz, we find $\lambda \approx$ 555.17 nm for the corresponding wavelength of the light source (green).

3. Blackbody radiation and the birth of quantum mechanics

To understand what motivated Planck to investigate the radiation entropy mentioned above, let's go back to the 19th century and examine one object that captivated Planck and so many other renowned physicists for several decades. In 1859, Gustav Kirchhoff coined the term "blackbody" to describe that object: a body that perfectly absorbs all thermal radiation falling upon it [2]. As is well known, black surfaces absorb light, they also absorb the greatest amount of thermal radiation. But there is another phenomenon associated with absorption which, in scientific terms, can be translated into the following statement: a surface in thermal equilibrium has an equal capacity of absorption and emission of thermal radiation; this relationship between absorption and emission is known as Kirchhoff's law of thermal radiation. Thus, a blackbody emits radiations whose characteristics are independent of the nature of the source of radiation and depend solely on its temperature. To demystify the blackbody, one can consider that solar radiation falling on the Earth closely approaches that of a blackbody in thermal equilibrium at 5777 K (≈ 5500 °C), as we shall see later. The importance of blackbody radiation is now obvious, as it is crucial for the understanding of thermal radiation and its laws.

From a practical perspective, in order to build a blackbody and be able to study it, one has to heat a cavity to a uniform temperature and allow the radiation to escape through a small aperture. As Kirchhoff had imagined in 1859, such a black cavity radiator is very close to an ideal blackbody. Yet, although simple in appearance, it was not until the close of the 19th century that a truly blackbody was designed at

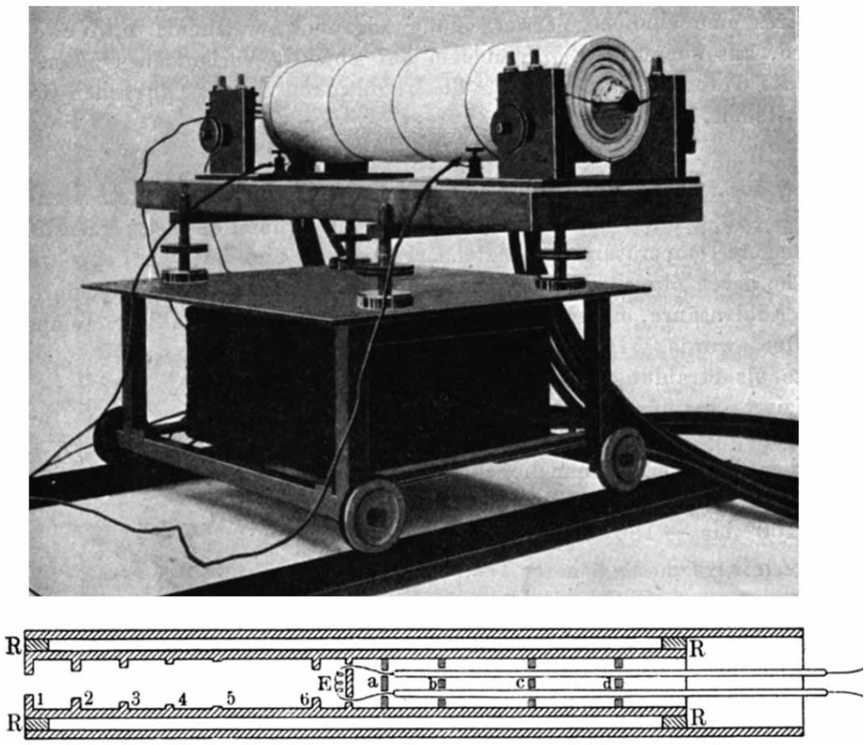

__Figure 1:__ The electrical glowing blackbody designed by O. Lummer and F. Kurlbaum in 1898 [2]. Current heats the filament located in a tube inside the cylinder to a fixed temperature, giving rise to blackbody radiation inside that cylinder. The spectrum of this radiation is observed through the hole found at one end along the axis of the cylinder. With a current of about 100 A, temperatures of about 1500 °C (1773 K) could be attained.

the Physikalisch – Technische Reichsanstalt (PTR) in Berlin (see Figure 1). There, blackbody radiation was a lively research topic for both experimental and theoretical physicists for two complementary reasons:

1. Practical (metrology) – The search for better standards (*e.g.*, absolute temperature scales), and in particular for a reliable standard for the radiation of light (radiometry).
2. Theoretical (radiation laws) – The construction of black cavities closely approaching blackbody radiation opened up a path to investigate the exact nature of radiation processes.

The apparatuses developed at the PTR meant great progress for radiation measurements. Experimental physicists could verify with precision measurements a law which had been empirically found by Joseph Stefan in 1879 and theoretically derived by Ludwig Boltzmann in 1884. The Stefan–Boltzmann law states that the radiant emittance, M_{e}, of a blackbody is proportional to the fourth power of its thermodynamic temperature T:

$$M_{\mathrm{e}} = \sigma T^4 \qquad [\mathrm{W.m^{-2}}] \text{ or } [\mathrm{kg.s^{-3}}] \qquad \textit{Eq. 1}$$

The constant of proportionality σ is called the Stefan–Boltzmann constant. Today, it can be calculated exactly from the SI defining constants introduced in Table 1:

$$\sigma = \frac{2\pi^5 k_{\mathrm{B}}^4}{15c^2h^3} \qquad [\mathrm{W.m^{-2}.K^{-4}}] \text{ or } [\mathrm{kg.s^{-3}.K^{-4}}] \qquad \textit{Eq. 2}$$

$$\sigma = 5.670\,374\,419 \ldots \times 10^{-8}\ \mathrm{W.m^{-2}.K^{-4}}$$

They could also conduct an experimental proof of Wien's displacement law that had been discovered by Wilhelm Wien. Wien's displacement law states that the blackbody radiation curve for different temperatures will peak at wavelengths that are inversely proportional to the temperature. When considering the spectral radiance of blackbody radiation per unit wavelength ($L_{\mathrm{e},\Omega,\lambda}$), it is found that it peaks at the wavelength:

$$\lambda_{\mathrm{pk}} = \frac{\sigma_{\mathrm{w}}}{T} \qquad [\mathrm{m}] \qquad \textit{Eq. 3}$$

The constant of proportionality σ_{w} is called Wien's displacement constant. It can be calculated exactly by solving a transcendental equation. Using the SI defining constants introduced in Table 1, an approximate value is:

$$\sigma_{\mathrm{w}} = \frac{hc}{4.965\,114\,231\,74\,k_{\mathrm{B}}} \qquad [\mathrm{m.K}] \qquad \textit{Eq. 4}$$

$$\sigma_{\mathrm{w}} = 2.897\,771\,955 \ldots \times 10^{-3}\ \mathrm{m.K}$$

More importantly, they were also able to test Wien distribution law of thermal radiation (now known as Wien's approximation). Using our current knowledge,[3] this law may be written in terms of the spectral energy density as a function of frequency ν:

$$u_\nu(\nu, T) = \frac{8\pi h\nu^3}{c^3} e^{\frac{-h\nu}{k_{\mathrm{B}}T}} \qquad [\mathrm{J.m^{-3}.Hz^{-1}}] \text{ or } [\mathrm{kg.m^{-1}.s^{-1}}] \qquad \textit{Eq. 5}$$

Alternatively, Wien's approximation can be written in terms of the spectral energy density as a function of wavelength $\lambda = c/\nu$:

$$u_\lambda(\lambda, T) = \frac{8\pi hc}{\lambda^5} e^{\frac{-hc}{\lambda k_{\mathrm{B}}T}} \qquad [\mathrm{J.m^{-3}.m^{-1}}] \text{ or } [\mathrm{kg.m^{-2}.s^{-2}}] \qquad \textit{Eq. 6}$$

The decisive contribution of the PTR team came from the tremendous refinement of their measurements at longer wavelengths. Indeed, the investigations revealed significant deviations from Wien's theoretical radiation at longer wavelengths. Conversely, a law that had been proposed earlier by John W. Rayleigh proved valid on long wavelengths but failed dramatically on short wavelengths (a divergence that would be coined the "ultraviolet catastrophe" by Paul Ehrenfest in 1911). This law, today known as the Rayleigh–Jeans law, can be obtained using only arguments from "classical" physics:

$$u_\nu(\nu, T) = \frac{8\pi k_{\mathrm{B}} T \nu^2}{c^3} \qquad [\mathrm{J.m^{-3}.Hz^{-1}}] \text{ or } [\mathrm{kg.m^{-1}.s^{-1}}] \qquad \textit{Eq. 7}$$

$$u_\lambda(\lambda, T) = \frac{8\pi k_{\mathrm{B}} T}{\lambda^4} \qquad [\mathrm{J.m^{-3}.m^{-1}}] \text{ or } [\mathrm{kg.m^{-2}.s^{-2}}] \qquad \textit{Eq. 8}$$

These contradictory results were presented by H. Rubens and F. Kurlbaum to the Prussian Academy in October 1900 and published one year after [3].

This work is considered to be the turning point in theoretical research on blackbody radiations. Indeed, it turns out that Rubens was a friend of Planck, as reported by the science historian A. Pais [4]. In the course of a conversation, Rubens mentioned to Planck that he had found $u_\lambda(\lambda, T)$ to be proportional to T for large wavelengths, *i.e.* in the infrared. In fact, it didn't take Planck long time to find a solution satisfying both Eq. 6 at short wavelengths and Eq. 8 at long wavelengths. Through interpolation, he found:

$$u_\lambda(\lambda, T) = \frac{8\pi hc}{\lambda^5} \frac{1}{e^{\frac{hc}{\lambda k_{\mathrm{B}}T}} - 1} \qquad [\mathrm{J.m^{-3}.m^{-1}}] \text{ or } [\mathrm{kg.m^{-2}.s^{-2}}] \qquad \textit{Eq. 9}$$

for the spectral energy density as a function of wavelength. Or, when expressed in terms of frequency instead of wavelength, using Eq. 5 and Eq. 7:

$$u_\nu(\nu, T) = \frac{8\pi h\nu^3}{c^3} \frac{1}{e^{\frac{h\nu}{k_{\mathrm{B}}T}} - 1} \qquad [\mathrm{J.m^{-3}.Hz^{-1}}] \text{ or } [\mathrm{kg.m^{-1}.s^{-1}}] \qquad \textit{Eq. 10}$$

[3] Of course, photon energy ($\varepsilon = h\nu$) didn't appear in this form in Wien's original equation since it was Planck who introduced energy quanta (see Appendix) and Einstein who introduced the concept of light quanta (see section 4).

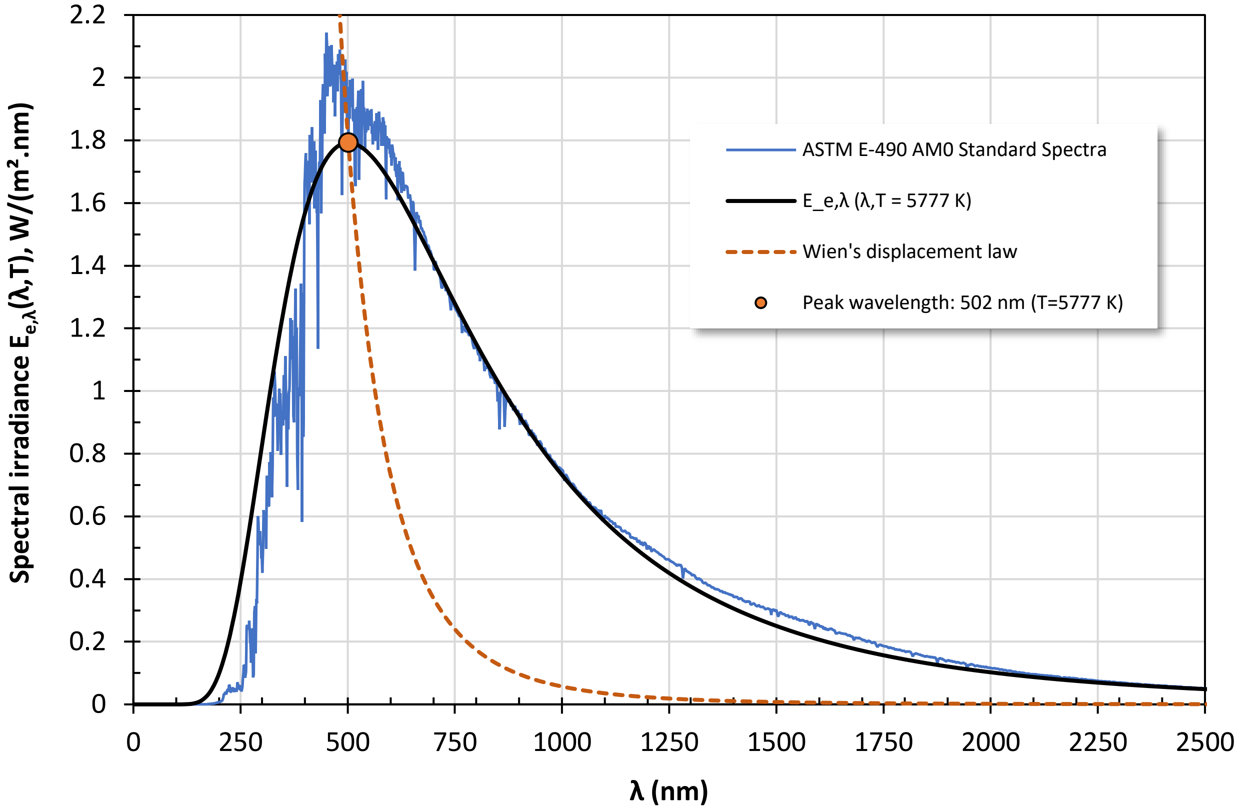

Figure 2: *Solar radiation spectrum is compared with a 5777 K blackbody (≈ 5500 °C). ASTM E-490 represents solar spectral irradiance above the atmosphere. For this temperature of the blackbody, Wien's displacement law predicts a peak wavelength around 500 nm.*

These two equations appear exactly in this form in Planck's famous paper "On the law of distribution of energy in the normal spectrum" published in 1901 [5].

Planck's discovery is by no means limited to an interpolation of experimental data. This was actually the starting point of the most heroic period of his life. Blackbody radiation involved an inescapable break with classical physics. As a physicist, he had to find a rational explanation. His law had to derive from a fundamental principle. He succeeded to give a physical explanation, but in order to do so he had to make the following hypothesis: radiation energy is found in the form of discrete energy elements ε – *i.e.*, quantized energy – that are proportional to the frequency ν:

$$\varepsilon = h\nu \qquad \text{[J] or [kg.m.s}^{-2}\text{]} \qquad \textit{Eq. 11}$$

For further details, readers will find in the Appendix a brief overview of the masterful demonstration that led Planck to the postulate of energy quanta.

To conclude this section on blackbody radiation, we show in Figure 2 the solar radiation spectrum as compared to a 5777 K blackbody (about 5500 °C). The ASTM E-490 solar spectral irradiance is based on a collection of data recorded above the atmosphere. Its integrated spectral irradiance has been made to conform to the value of the solar constant accepted by the space community, which is 1366.1 W/m². The spectral irradiance $E_{e,\lambda}$ is calculated from the spectral energy density u_λ given in Eq. 6:

$$E_{e,\lambda}(\lambda, T) = c\,\frac{\Omega_{\text{Sun}}}{4\pi}\,u_\lambda(\lambda, T) \qquad \text{[W/(m}^2\text{.m)]} \qquad \textit{Eq. 12}$$

with $\Omega_{\text{Sun}} \approx 6.807\times10^{-5}$ sr, the solid angle of the Sun as seen from Earth.[4] Although the Sun is not a perfect blackbody, we can see a relatively good correspondence with the 5777 K blackbody. According to Wien's displacement law (Eq. 3), the peak wavelength of the 5777 K blackbody is around 502 nm:

$$\begin{aligned} \lambda_{\text{pk}} &= \sigma_{\text{w}} \,/\, (5777\ \text{K}) \\ &\approx 5.016\times10^{-7}\ \text{m} \\ &\approx 502\ \text{nm} \end{aligned}$$

[4] The Sun as seen from Earth has an average apparent angular diameter of $2\theta_{\text{Sun}} \approx 0.5334°$. The corresponding solid angle is $\Omega_{\text{Sun}} = 2\pi\,(1 - \cos(\theta_{\text{Sun}}))$, expressed in steradian [sr].

4. Photoelectric effect

After 1901, nothing further happened in quantum mechanics until Albert Einstein proposed the light quantum hypothesis in 1905 [5]. Einstein's greatest strength laid in tracking down fruitful ideas from the scientific literature, then to draw together these isolate insights into consistent theories [5]. This way of thinking forms the framework of his paper "On a heuristic point of view concerning the generation and conversion of light" [6], [7]. This is how he came up with the first quantum theory of radiation. At this point, it should be noted that the word "photon" – which denotes the particle nature of light – did not appear until 1926, after the wave-particle duality had been clarified.

Planck had proposed Eq. 11 in 1901 but it was only an ad-hoc assumption. As Planck conceded, it was supposed to be a mathematical artifact. Meanwhile, Philippe Lenard was working on "cathode rays" and encountered various difficulties when attempting to explain photoelectric phenomena, that is the emission of electrons (photoelectrons) when light hits a material. Lenard found that the electron energy showed "not the slightest dependence on the light intensity" [3]. On the other hand, he could observe that photoelectron energy did increase with the frequency ν of monochromatic light.

Einstein then proposed the following picture for the photoelectric effect. A light quantum of frequency ν transfers all its energy to a single electron, independently of the presence of other light quanta. The electron can suffer energy loss before it reaches the surface. When ejected from the surface of the material, electron energy is found as kinetic energy and can reach E_{kmax}. In the case where this energy loss is zero, he translated the photoelectric effect into the following equation (in modern notation):

$$E_{kmax} = h\nu - \varphi \qquad \text{Eq. 13}$$

where φ is the work function of the material, i.e. the energy needed to escape the surface. Eq. 13 explains Lenard's observation of the electron energy being independent of the light intensity. With this equation, Einstein made several strong predictions:

i) linear dependence of E_{kmax} with ν

ii) the slope h is the Planck constant; it is thus independent of the material

iii) the work function is a material dependent property

iv) one can define $\nu_{th} = \varphi/h$, a threshold frequency of light below which no photoelectric effect is observed.

As an illustrative example, let's consider light incident on a silver (Ag) plate. The work function of silver, φ_{Ag}, is around 4.3 eV (electron-volt[1]):

$$\begin{aligned}\varphi_{Ag} &= 4.3\ \text{eV} \\ &= 4.3 \times 1.602\,176\,634 \times 10^{-19}\ \text{J or [C.V]} \\ &= 6.89 \times 10^{-19}\ \text{J}\end{aligned}$$

The threshold wavelength, λ_{th}, above which no photoelectric effect is observed is:

$$\begin{aligned}\lambda_{th} &= \frac{c}{\nu_{th}} = h.c/\varphi_{Ag} \\ &= 2.88 \times 10^{-7}\ \text{m} \\ &= 288\ \text{nm}\end{aligned}$$

The threshold wavelength is in the deep ultraviolet. In other words, nothing happens when visible light hits silver: visible light does not have enough energy to free an electron from silver.

5. Semiconductor photonic devices

The discovery of the photoelectric effect and the advances in quantum physics were a prerequisite to the construction of semiconductor photodetectors – commonly referred to as photodiodes – and light-emitting diodes (LEDs). We know from quantum physics that the energy of an electron in an atom is quantized. In a solid, the interatomic interaction results in the formation of energy bands. These energy bands can overlap, as is the case in metals. However, there are certain materials known as semiconductors were the interaction between atoms and their valence electrons (outer shell electrons) results in two very close but distinct energy bands. They are called the valence band (energy E_v) and the conduction band (energy E_c) and are separated by an energy gap, or energy "bandgap" E_g:

$$E_g = E_c - E_v \qquad \text{Eq. 14}$$

This bandgap represents forbidden electron energies in the material. As a result, semiconductors have a very distinctive electrical characteristic that changes depending on the environment. They owe their name to the fact that their conductive behaviour lies between that of a conductor and an insulator. For instance, silicon (Si) crystal – a pure or "intrinsic" semiconductor – is an insulator at room temperature but becomes slightly conductive when heated. Of course, there are other more effective ways of changing semiconductors conductivity, for instance by using light, an electric current, a magnetic field or an electric field.

[1] The electron-volt (eV) is a convenient alternative to the joule (J). It is calculated from the elementary charge, e (C): 1 eV = 1.602 176 634 ×10⁻¹⁹ J. Note that [J] = [C.V].

Table 2: Typical energy band gap of some semiconductor materials

Material	Energy bandgap [a] (E_g) at room temperature, typ.	Cutoff wavelength (λ_g)
Aluminium Nitride (AlN)	6.0 eV, direct	200 nm
Gallium Nitride (GaN)	3.4 eV, direct	365 nm
Gallium Phosphide (GaP)	2.26 eV, indirect	550 nm
Silicon (Si)	1.12 eV, indirect	1100 nm
Germanium (Ge)	0.67 eV, direct	1850 nm
Indium Nitride (InN)	0.65 eV, direct	1900 nm

a) Indirect bandgap semiconductors, such as silicon, cannot be directly used to make LEDs.

Doping, i.e. the introduction of foreign atomic species (impurities), is another way to locally change a semiconductor conductivity. It is the basic process for the manufacture of the so-called "extrinsic" semiconductor devices. Current conductivity in a doped semiconductor is enhanced due to mobile charge carriers, which are either electrons or electron "holes" (the lack of electrons). When a doped semiconductor contains excess holes, it is called a p-type material (p stands for positive electric charges); when it contains excess free electrons, it is called an n-type material (negative). A p-n junction is formed when the n- and p-type semiconductors have intimate contact. The p-n junction is the building block of semiconductor devices: a diode, a photodiode and a light-emitting diode (LED) can be made from a single p-n junction.

At the p-n junction, electrons and holes diffuse to recombine with each other. This creates a region without charge carriers, a depletion. At the depletion, a built-in electric field is obtained which acts as a barrier to the movement of electrons. This implies that a voltage at least equal to the potential barrier, V_{bi}, must be applied across the p-n junction in order for the electrons to move through this electric field [8]. In a photonic device, when an electron jumps this energy, it can result either in the emission or in the absorption of a photon:

electron + hole ⇌ photon

In a photodiode, the absorption of a photon results in a free electron-hole pair, that is the creation of an electron in the conduction band and the creation of a hole in the valence band. Whether a photodiode or an LED, the photoelectron or the emitted photon must have an energy equal to ΔE, the energy difference between the conduction band electron and the valence band hole that participated in the process [9]. As a first approximation, we may write:

$$\Delta E = E_g \qquad \text{Eq. 15}$$

Energy ΔE may also be written as a function of the voltage V across the p-n junction (see also footnote 5):

$$\Delta E = eV \qquad \text{Eq. 16}$$

Due to the conservation of energy, the electron energy eV equals the photon energy $h\nu$ (see Eq. 11):

$$eV = h\nu \qquad \text{Eq. 17}$$

Beyond activation, the voltage V across the device is about the same as the potential barrier V_{bi}, thus:

$$V_{bi} = \frac{h\nu}{e} \quad [V] \qquad \text{Eq. 18}$$

Combining these equations, we finally find the characteristic wavelength λ_g:

$$\lambda_g = \frac{hc}{E_g} \qquad \text{Eq. 19}$$

This wavelength is known as the cutoff wavelength for photodiodes [10], while it approximates the peak emission wavelength of an LED [9]. For example, in the case of silicon, the bandgap energy is around 1.12 eV, so the cutoff wavelength of an Si photodiode is around 1100 nm (see Table 2). This means that an Si photodiode can be used to detect photons whose wavelength is lower than 1100 nm.

As we are concerned with the spectral distribution of LEDs, an important remark must be given concerning the approximation made at Eq. 15. Although the nominal photon energy ΔE is in the vicinity of the material bandgap E_g, its distribution depends on the width of the associated energy bands and on the statistical distribution of free carriers within these bands. In concrete terms, since LEDs are semiconductor materials that have energy bands instead of discrete energy levels as in the case of gases, free carrier transition between these energy bands allows photon emission in a relatively wide wavelength window [9]. For a given peak emission wavelength, an LED will show a relatively broader emission spectrum as compared to that achievable with a corresponding gas-discharge lamp. On the other hand, LED spectrum is well-delimited as opposed to the continuum radiation of gas-discharge lamps. This is illustrated in Figure 3 which compares the spectral power distribution (SPD) of an ultraviolet (UV) "365 nm" UV-LED with that of a mercury-vapor lamp (Hg).

6. Photodiode responsivity

From sections 4 and 5, it follows that when the wavelength is too long and the photon energy is too low, the response of a photodetector will drop to zero if the necessary condition $h\nu \geq E_g$ is not satisfied. Let's see what happens when this condition is satisfied. The absorbed photons create photoelectrons that can be

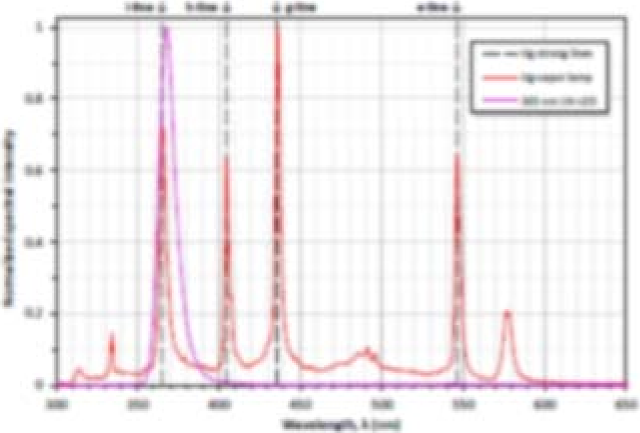

Figure 3: Spectral power distribution of a "365 nm" UV-LED lamp is compared with that of a mercury-vapor lamp. Both spectra were acquired with an extended range spectrometer (FLAME-S-XR1-ES, Ocean Insight, Inc.)

collected and give rise to a photocurrent, I_{ph}. From the definition of the ampere, $[A] = [C.s^{-1}]$, the number of electrons collected per second is I_{ph}/e. The total optical power (or radiant flux) incident on the photodiode is Φ_e and is measured in watts, $[W] = [J.s^{-1}]$. Similarly to what we did in section 3, we use the subscript λ for the radiant flux per unit wavelength (spectral flux), $\Phi_{e,\lambda}$. It has units of watts per meter, $[W.m^{-1}] = [J.s^{-1}.m^{-1}] = [kg.m.s^{-3}]$. With this formalism, we can now express the number of photons received per seconds for a given wavelength: $\Phi_{e,\lambda}\lambda/(hc)$.

Not all the photons are absorbed and converted into photocurrent. The efficiency of this conversion is measured by the quantum efficiency (QE) of the photodetector, η_{QE}:

$$\eta_{QE} = \frac{\text{No. generated electron-hole pairs}}{\text{No. incident photons}} \qquad \text{Eq. 20}$$

This expression can be rewritten as:

$$\eta_{QE} = \frac{I_{ph}/e}{\Phi_{e,\lambda}\lambda/(hc)} = \frac{I_{ph}}{\Phi_{e,\lambda}}\frac{hc}{e\lambda} \qquad \text{Eq. 21}$$

The ratio $I_{ph}/\Phi_{e,\lambda}$ is called the spectral responsivity $\Re$ of a photodiode. It characterises the photodiode performance in terms of photocurrent per incident optical power at a given frequency (spectral flux):

$$\Re(\lambda) = \frac{I_{ph}(\lambda)}{\Phi_{e,\lambda}(\lambda)} \qquad [A/W] \qquad \text{Eq. 22}$$

From the definition of QE given in Eq. 21, it follows that:

$$\Re = \eta_{QE}\frac{e}{h\nu} = \eta_{QE}\frac{e\lambda}{hc} \qquad [A/W] \qquad \text{Eq. 23}$$

Because QE depends on the wavelength, $\Re$ is therefore clearly dependent on the wavelength.

We can now give the responsivity of a photodiode as a function of the wavelength λ, considering the cutoff wavelength λ_{co} given in Eq. 13:

$$\begin{cases} \Re(\lambda < \lambda_{co}) = \eta_{QE}\frac{e\lambda}{hc} \\ \Re(\lambda \geq \lambda_{co}) = 0 \end{cases} \qquad \text{Eq. 24}$$

The characteristic $\Re(\lambda)$ represents the spectral response of the photodiode and can be found in the manufacturer's datasheet. Figure 4 shows the typical responsivity of a silicon photodiode as compared with its ideal theoretical model. In the ideal case, the responsivity increases linearly with the wavelength and then suddenly drops at the cutoff wavelength λ_{co}. In

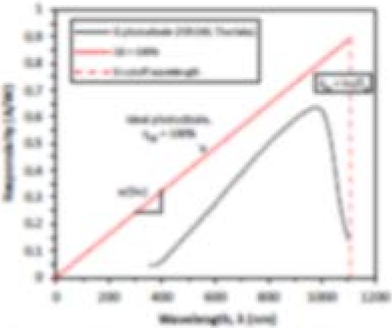

Figure 6: The spectral responsivity of an ideal photodiode (quantum efficiency QE = 100%) is compared with that of a commercial silicon photodiode (model FDS100, Thorlabs, Inc.)

practice QE < 100% and the responsivity curves is found to lie below the ideal curve. This being said, one should note that the spectral response of Si-based photodiodes covers the entire visible spectrum. Furthermore, its linearity is remarkable for wavelengths in the visible range, which makes Si a suitable candidate for visible light radiometry.

7. Spectral power distribution of a light-emitting diode

We concluded section 5 by pointing out that, due to the widths of the energy bands and to the statistical distribution of free carriers, the spectral power distribution (SPD) of LEDs is a relatively wide emission around a peak emission wavelength. As can be seen in Figure 5, this SPD may be approximated as an asymmetric gaussian curve. This asymmetry is more or less pronounced and depends on the composition of the semiconductor material. Thanks to the knowledge disseminated so far, a more in-depth interpretation of this SPD is now at hand.

To describe LED emission spectrum, Würfel proposed a generalisation of Planck's law of radiation [11], [12], [13]. By introducing a non-zero "chemical potential" of photons, he showed that the light emitted by LEDs can be well described by a thermodynamic theory extending Planck's law to luminescent radiation. Using the notation introduced in section 3, the spectral energy density as a function of photon frequency rewrites as follows:

$$u_\nu(\nu,T) = a_\nu(h\nu)\frac{8\pi\nu^2}{c^3}\frac{h\nu}{e^{\frac{h\nu-\mu_\gamma}{kT}}-1} \qquad \text{Eq. 25}$$

with Eq. 10. Because a blackbody is an ideal object that has perfect absorption, its surface absorptivity is always 1, so $a_\nu(h\nu) = 1$. Next, blackbody radiation describes the states of light in which the chemical potential is zero [12], so $\mu_\gamma = 0$.

In solid-state lighting devices such as LEDs, light is produced with a non-zero chemical potential by using chemical equilibrium with the excited matter. Contrary to a blackbody, LED light has a temperature not far from room temperature, and its chemical potential is greater than zero, $\mu_\gamma > 0$. The temperature T is that of the electron-hole gas, which is equal to the semiconductor junction temperature. The chemical potential is equal to that of the electron-hole pair, which is determined by the voltage V across the p-n junction: $\mu_\gamma = eV$ [13]. In semiconductors, this electrochemical potential μ_γ is known as the quasi-Fermi level splitting.

Here, we observe that Eq. 25 seems to diverge at $h\nu = \mu_\gamma$, which of course doesn't happen in practice. This apparent inconsistency is resolved by noting that the energy-dependent factor $a_\nu(h\nu)$ holds information about carriers' density of states. In an idealised LED, $a_\nu(h\nu)$ is a step function: photons with energy smaller than the bandgap energy cannot be absorbed by generating electron-hole pairs, resulting in $a_\nu(h\nu < \mu_\gamma) = 0$, whereas all photons with energy higher than the bandgap energy are fully absorbed, $a_\nu(h\nu > \mu_\gamma) = 1$ [12]. From these considerations, Würfel postulates that, for LEDs, the −1 in the denominator of Eq. 25 can be neglected [12], [13]. As a result, Eq. 25 may be approximated by:

$$u_\nu(\nu,T) = a_\nu(h\nu)\,\frac{8\pi h\nu^3}{c^3}\,e^{-\frac{h\nu}{kT}}\,e^{\frac{\mu_\gamma}{kT}} \qquad \text{Eq. 26}$$

This relation can be regarded as Wien's generalised law of radiation applied to LEDs (see Eq. 9 for comparison). Light emission above the bandgap energy can be thought of as Planckian radiation exponentially enhanced by diode voltage [11].

Eq. 26 predicts that the light emitted by a LED is fully described by the absorptivity, the applied voltage and the junction temperature. Absorptivity is definitely the most complex part of this equation as it depends on the internal composition of the p-n junction (e.g., spatial

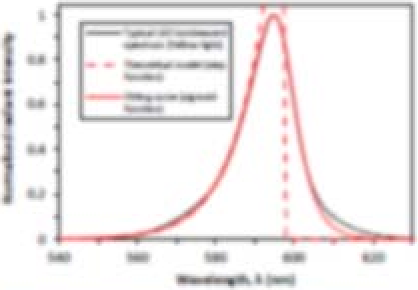

Wavelength, λ (nm)

Table 3: This octave script computes a fitting algorithm from raw data of a LED spectral power distribution

```
% Fitting algorithm: compatible with GNU Octave
% Data are loaded from a CSV file (e.g., "LED_spectrum.csv").
%
% CSV stands for "comma-separated values"
% The CSV consists of ASCII data: X and Y data arranged in two columns
% Values can be delimited either with a comma (,) or a semicolon (;).

clear;

% Load X and Y values
data = dlmread('LED_spectrum.csv');
xdata = data(:,1);
ydata = data(:,2);

% Define the model. Here, we use a sum of gaussian functions for the fitting
model_func = @(p) sum((ydata ...
  - (p(1).*exp(-0.5*((xdata-p(2)) / p(3)).^2) ...
  +  p(4).*exp(-0.5*((xdata-p(5)) / p(6)).^2) ...
  +  p(7).*exp(-0.5*((xdata-p(8)) / p(9)).^2))).^2);

% Function to evaluate the model. In this case, we need to provide
% the error function: residual sum of squares (RSS)
RSS_func = @(p, x) ...
      p(1).*exp(-0.5*((x-p(2)) / p(3)).^2) ...
  +  p(4).*exp(-0.5*((x-p(5)) / p(6)).^2) ...
  +  p(7).*exp(-0.5*((x-p(8)) / p(9)).^2);

% Initial guess
p_init = [1, 445, 5, 0.5, 575, 15, 0.1, 500, 20];

% Nonlinear fit: fitting parameters are displayed in the Command Window
fitting_parameters = fminsearch(model_func, p_init)'

% A graph is displayed
plot(xdata, ydata, 'bo');
fig = gcf ();
set (fig, "numbertitle", "off", ...
   "name", "Data fitting with a sum of gaussian functions");
hold on
plot(xdata, RSS_func(fitting_parameters', xdata), ...
   'r', 'linewidth', 2);
xlabel('Wavelength, \lambda (nm)');
ylabel('Spectral irradiance, E_{e,\lambda}(\lambda) (a.u.)');
```

$$\Phi_e = \int_0^\infty \Phi_{e,\lambda}(\lambda)d\lambda = A_1\sigma_1\sqrt{2\pi} \qquad \text{Eq. 31}$$

A simple gaussian is clearly not a satisfying approximation. The actual spectrum being asymmetrical, the fitting is instead completed with two gaussian functions and we obtain:

$$\begin{aligned}\Phi_e &= A_1 \int_0^\infty e^{-\frac{1}{2}\left(\frac{\lambda-\lambda_1}{\sigma_1}\right)^2} + A_2 \int_0^\infty e^{-\frac{1}{2}\left(\frac{\lambda-\lambda_2}{\sigma_2}\right)^2} \\ &= A_1\sigma_1\sqrt{2\pi} + A_2\sigma_2\sqrt{2\pi}\end{aligned} \qquad \text{Eq. 32}$$

We rewrite the radiant flux as:

$$\Phi_e = \Phi_{e,1} + \Phi_{e,2} \qquad \text{Eq. 33}$$

where $\Phi_{e,1} = A_1\sigma_1\sqrt{2\pi}$ and $\Phi_{e,2} = A_2\sigma_2\sqrt{2\pi}$.

We now introduce the centroid wavelength, λ_c, which is ideal for characterising the asymmetrical SPD of LEDs. It is calculated as follows:

$$\lambda_c = \frac{\int_0^\infty \lambda\cdot\Phi_{e,\lambda}(\lambda)d\lambda}{\int_0^\infty \Phi_{e,\lambda}(\lambda)d\lambda} = \frac{\int_0^\infty \lambda\cdot\Phi_{e,\lambda}(\lambda)d\lambda}{\Phi_e} \qquad \text{Eq. 34}$$

It can be easily shown that Eq. 34 can be rewritten as follows:

$$\lambda_c = \frac{\lambda_1\Phi_{e,1} + \lambda_2\Phi_{e,2}}{\Phi_{e,1} + \Phi_{e,2}} \qquad \text{Eq. 35}$$

This relation clearly shows that the centroid wavelength is analogous to the barycentre of the spectrum.

We want to characterise the LED with a photodiode. As we learned in section 3, the responsivity $\Re(\lambda)$ of a photodiode is the ratio of the generated photocurrent, $I_{ph}(\lambda)$, to the incident spectral flux at a given wavelength, $\Phi_{e,\lambda}(\lambda)$:

$$\Re(\lambda) = \frac{I_{ph}(\lambda)}{\Phi_{e,\lambda}(\lambda)} \qquad \text{Eq. 36}$$

This result is similar to Eq. 22 but involves wavelength-dependent quantities. When integrated in a radiometer, the photocurrent delivered by the photodiode is amplified and converted. The output signal, I, of the radiometer is obtained through integration of the responsivity times the spectral flux over the entire bandwidth [16]:

$$I = k \int_0^\infty \Re(\lambda) \cdot \Phi_{e,\lambda}(\lambda)\, d\lambda \qquad \text{Eq. 37}$$

where k is a constant specific to the radiometer. As we have seen in Figure 4, the radiometer has a non-flat spectral responsivity. However, it can suitably be used for metrology if the responsivity can be linearised around the LED peak (ideally, at least beyond twice the FWHM). In this case, we have:

$$\Re(\lambda) = \alpha \cdot \lambda + \beta \qquad \text{Eq. 38}$$

where α and β are two constants. At the centroid wavelength, we then find:

$$\Re(\lambda_c) = \alpha \cdot \lambda_c + \beta \qquad \text{Eq. 39}$$

The slope, α, can be rewritten as follows:

$$\alpha = \frac{\Re(\lambda_2) - \Re(\lambda_1)}{\lambda_2 - \lambda_1} \qquad \text{Eq. 40}$$

We deduce the following relation:

$$\begin{aligned} &\int_0^\infty \Re(\lambda) \cdot \Phi_{e,\lambda}(\lambda)\, d\lambda \\ &= \int_0^\infty (\alpha \cdot \lambda + \beta) \cdot \Phi_{e,\lambda}(\lambda)\, d\lambda \\ &= \alpha \int_0^\infty \lambda \cdot \Phi_{e,\lambda}(\lambda) d\lambda + \beta \int_0^\infty \Phi_{e,\lambda}(\lambda)\, d\lambda \end{aligned} \qquad \text{Eq. 41}$$

Thus, we have:

$$\begin{aligned} &\int_0^\infty \Re(\lambda) \cdot \Phi_{e,\lambda}(\lambda)\, d\lambda \\ &= \alpha \lambda_c \Phi_e + \beta \Phi_e = \Re(\lambda_c) \cdot \Phi_e \end{aligned} \qquad \text{Eq. 42}$$

Combining Eq. 42 with Eq. 37, we obtain:

$$I = k \cdot \Re(\lambda_c) \cdot \Phi_e \qquad \text{Eq. 43}$$

This result demonstrates that the radiant flux Φ_e of a single-peaked LED can be properly estimated with a non-flat radiometer provided that the photodiode used can be linearised around the centroid wavelength λ_c of the LED. In this case, the calibration parameter to be used is $\Re(\lambda_c)$, the responsivity of the photodiode at λ_c.

Furthermore, there is another important result that arises from the above as it can be straightforwardly shown that:

$$\Re(\lambda_c) \cdot \Phi_e = \Re(\lambda_1) \cdot \Phi_{e1} + \Re(\lambda_2) \cdot \Phi_{e2} \qquad \text{Eq. 44}$$

Indeed, Eq. 44 implies that a radiometer – calibrated for centroid wavelength λ_c – provides the same output signal as if it were used to measure separately the distinct gaussian spectra at wavelengths λ_1 and λ_2, respectively. In other words, the methodology described above can be generalised to the radiometric measurement of multi-peak LEDs, i.e. broadband spectrum obtained from the combination of several gaussian spectra. In that case, the photodiode must be linearisable throughout the entire bandwidth.

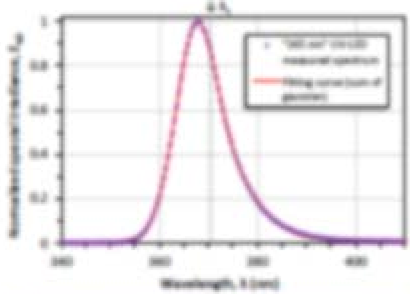

Figure 6: Normalised spectral irradiance of a "365 nm" UV-LED and the fitting curve obtained using the algorithm detailed in Table 2. The measured SPD is the same as that shown in Figure 3. Note that the centroid wavelength λ_c is slightly shifted with respect to the peak wavelength.

In Figure 7, we have reproduced the normalised responsivity of a Gallium Phosphide (GaP) photodiode together with the normalised SPD of a multi-peak UV-LED. In this illustrative example, the LED spectrum was fitted with three gaussian curves. It can be seen that the responsivity of GaP shows good linearity over the entire spectrum of the LED (i.e., 350 nm – 450 nm). The solid curve displayed on

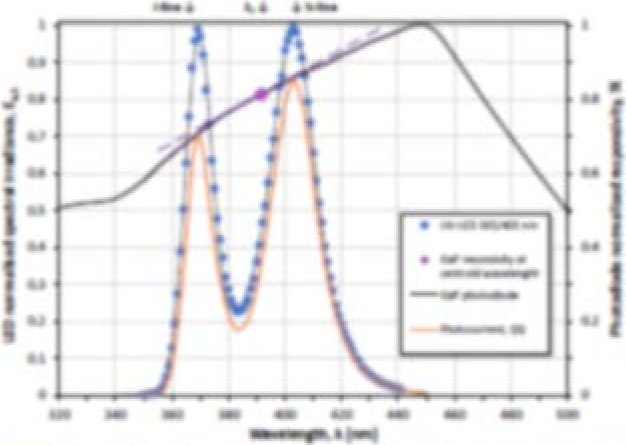

Figure 7: Normalized spectral irradiance of a multi-peak UV-LED vs. typical responsivity of Gallium Phosphide (GaP) photodiode. The solid curve (I) is the calculated wavelength dependent photocurrent. GaP responsivity can be linearized in the near UV range, making GaP semiconductor a suitable radiometric sensor for this UV-LED.

the graph was calculated as $I(\lambda) = R(\lambda) \cdot \Phi_{e,\lambda}(\lambda)$ by data interpolation. Clearly, from Eq. (7), one can immediately see that the output signal of the photodiode is obtained through integration of the latter curve. As demonstrated above (see Eq. (6)), the radiant flux Φ_e can directly be retrieved from the radiometer provided that the centroid wavelength λ_c is used for the responsivity, $R(\lambda_c)$. Through numerical integration of the data displayed in Figure 7, we find that the estimation error is <1% when λ_c is used to calculate the responsivity. The radiant flux is overestimated by almost +11% if the i-line peak (365 nm) is used, while it is underestimated by about -4% if the h-line peak (405 nm) is used. These errors can easily be retrieved if one observes the relative responsivities of GaP at these wavelengths.

The experiments carried out with a spectrometer and a GaP photodiode corroborate the theoretical prediction that the photodiode can be used as a reliable radiometric sensor for the characterization of broadband LEDs. This is owed to the linearity of photodiode responsivity, which must of course be verified throughout the entire spectrum of the LED or group of LEDs of interest. To use a calibrated photodiode as a radiometer for LEDs, the centroid wavelength of its spectrum is then the only parameter that needs to be known to properly scale the output signal. The premises of such idea can be found in studies conducted by Eppeldauer et al. from the National Institute of Standards and Technology (NIST, USA) [18], [19]. However, these studies focused on single-peaked 365 nm UV-LED and considered the peak wavelength instead of the more suitable centroid wavelength. As a last remark, note that: (i) the typical peak wavelength of LEDs is always mentioned in their datasheets; (ii) the centroid wavelength is usually provided for LEDs emitting in the non-visible spectrum (infrared or ultraviolet). One should not use the "dominant wavelength" usually provided for LEDs emitting in the visible spectrum: this is a photometric value that calculates the apparent color, as perceived by the average human eye.

8. Conclusion

We began this white paper by emphasizing on the importance of accurate and precise measurements for science and technology. This assertion is a fortiori applicable to radiometric measurement and motivated the writing of this white paper whose primary aim was to demonstrate the reliability of radiometric measurement of LEDs using a simple photodiode. The proof can be summarised in two main points:

1. The electroluminescence spectrum of a LED can be approximated by a sum of gaussian curves from which a centroid wavelength λ_c can be derived;
2. By appropriate choice of a photodiode (*i.e*, with a linearizable responsivity $\Re(\lambda)$ throughout the entire bandwidth of the LED), its output signal gives a correct radiometric measurement of the LED provided scaling by its responsivity at centroid wavelength, $\Re(\lambda_c)$.

This is detailed in section 8 and we could have limited this paper to that section. However, we wanted to take the investigation on LEDs spectra a step further and explain the origin of their asymmetric gaussian-like shape.

One thing leading to another, what we did out of scientific curiosity eventually led us to dig in history of science, with blackbody radiation as the starting point. As we have stressed it in section 3, it was indeed the need for reliable standard for the radiation of light that prompted standardisation institutes to take an interest in blackbody radiation at the end of the 19th century. In light of what we have seen throughout this paper, the blackbody is in many ways essential to the understanding of quantum photonic devices, and LEDs in particular. Since we have developed the subject from a historical perspective, this has led us to mention several renowned scientists, including Nobel Prize laureates from the 20th century. It is therefore logical that we conclude this paper by recalling that the Nobel Prize in Physics 2014 was awarded jointly to Isamu Akasaki, Hiroshi Amano and Shuji Nakamura "for the invention of efficient blue light-emitting diodes which has enabled bright and energy-saving white light sources." The Nobel committee was not mistaken: LED technology has a bright future ahead of it!

Appendix: Planck's steps to the discovery of quantum theory

Planck wanted to interpret Eq. 10 which he had discovered empirically. His original derivation of that equation made him the discoverer of quantum theory [21]. To appreciate the importance of his work, we shall outline the three steps he took.

1. Classical electromagnetic theory

First, he established the relation:

$$u_\nu(\nu, T) = \frac{8\pi\nu^2}{c^3} U_\nu(\nu, T) \qquad \text{Eq. 45}$$

between the energy density u_ν of the equilibrium radiation at temperature T and the average energy U_ν of a resonator of frequency ν and temperature T. He completed this proof on the basis of classical electromagnetic theory. Comparing Eq. 10 and Eq. 45, he could then find U_ν:

$$U_\nu(\nu, T) = \frac{h\nu}{e^{\frac{h\nu}{k_B T}} - 1} \qquad \text{Eq. 46}$$

2. Thermodynamics and entropy

Planck was a convinced promoter of entropy. In the second step, he determined the entropy, S, of the resonators by integration of $T\mathrm{d}S = \mathrm{d}U$. From Eq. 46, he evaluated T as a function of U_ν for a fixed frequency ν. He obtained:

$$S = k_B \left[\left(1 + \frac{U_\nu}{h\nu}\right) \ln\left(1 + \frac{U_\nu}{h\nu}\right) - \frac{U_\nu}{h\nu} \ln \frac{U_\nu}{h\nu}\right] \qquad \text{Eq. 47}$$

3. Statistical thermodynamics

The third step was the revolutionary one. To complete this ultimate stage, he drew heavily on Boltzmann's work on statistics and entropy [22], [23]. To this end, he considered a system of N resonators vibrating at frequency ν. The total energy of these oscillators is $U_N = N\, U_\nu$, to which corresponds a total entropy $S_N = N\, S$. In an "act of desperation", as he would qualify it later, he then made the *ad hoc* assumption that the total energy was made up of finite energy elements ε, such that $U_N = P\,\varepsilon$, with P a large integer.

He followed one of Boltzmann's ideas according to whom entropy, apart from an additive constant, is proportional to the logarithm of the number W of "complexions" that constitute the equilibrium state of the system. Although Boltzmann never wrote down the equation, Planck formulated it as follows:

$$S_N = k_B \ln(W) + \text{const.} \qquad \text{Eq. 48}$$

Then, he calculated the number W of "complexions" (or permutations in combinatorics)[6] for a discrete system consisting of P energy elements that are distributed between N resonators:

$$W = \frac{(N + P - 1)!}{(N - 1)!\, P!} \qquad \text{Eq. 49}$$

Applying Stirling's formula,[7] he found:

$$W \approx \frac{(N + P)^{N+P}}{N^N P^P} \qquad \text{Eq. 50}$$

[6] Planck chose the symbol W, which is the first letter of "Wahrscheinlichkeit", the German word for probability.

[7] $\ln(N!) = N\ln(N) - N$

Finally, using $P/N = U_\nu/\varepsilon$ and $S = S_N/N$, he obtained:

$$S = k_\mathrm{B}\left[\left(1+\frac{U_\nu}{\varepsilon}\right)\ln\left(1+\frac{U_\nu}{\varepsilon}\right) - \frac{U_\nu}{\varepsilon}\ln\frac{U_\nu}{\varepsilon}\right] \qquad \textit{Eq. 51}$$

Since entropy only depends on U_ν/ν according to Wien's displacement law, it follows from the comparison of Eq. 47 and Eq. 51 that

$$\varepsilon = h\nu \qquad \textit{Eq. 52}$$

This is how quantum theory was born. Planck has been quite criticized for his audacity on this third step, especially for his use of Eq. 49 for which he had no justification, except that it was giving him the result he was looking for...

References

[1] M. Planck, "Über irreversible Strahlungsvorgänge," *Annalen der Physik,* vol. 360, no. 1, pp. 69-122, 1900.

[2] D. Hoffmann, "On the experimental context of Planck's foundation of quantum theory," *Centaurus,* vol. 43, no. 3-4, pp. 240-259, 2001.

[3] H. Rubens and F. Kurlbaum, "On the Heat Radiation of Long Wave-Length Emitted by Black Bodies at Different Temperatures," *Astrophysical Journal,* vol. 14, pp. 335-348, 1901.

[4] A. Pais, Subtle Is the Lord: The Science and the Life of Albert Einstein, Oxford University Press, 1982.

[5] M. Planck, "Über das Gesetz der Energieverteilung im Normalspectrum," *Annalen der Physik,* vol. 309, no. 3, pp. 553-563, 1901.

[6] A. Einstein, "Über einen die Erzeugung und Verwandlung des Lichtes betreffenden heuristischen Gesichtspunkt," *Annalen der Physik,* vol. 322, no. 6, pp. 132-148, 1905.

[7] K. Hentschel, "Light quantum," in *Compendium of Quantum Physics*, Berlin, Heidelberg, Springer, 2009, pp. 339-346.

[8] A. B. Arons and M. B. Peppard, "Einstein's Proposal of the Photon Concept — a Translation of the Annalen der Physik Paper of 1905," *American Journal of Physics,* vol. 33, no. 5, pp. 367-374, 1965.

[9] E. F. Schubert, J. Cho and J. Kim, "Light emitting diodes," in *Encyclopedia of Condensed Matter Physics*, Academic Press, 2016, pp. 102-111.

[10] R. Hui, "Light sources for optical communications," in *Introduction to Fiber-Optic Communications*, Academic Press, 2020, pp. 77-124.

[11] R. Hui, "Photodetectors," in *Introduction to Fiber-Optic Communications*, Academic Press, 2020, pp. 125-154.

[12] P. Würfel, "The chemical potential of radiation," *Journal of Physics C: Solid State Physics,* vol. 15, no. 18, pp. 3967-3985, 1982.

[13] F. Herrmann and P. Würfel, "Light with nonzero chemical potential," *American Journal of Physics,* vol. 73, no. 8, pp. 717-721, 2005.

[14] B. Feuerbacher and P. Würfel, "Verification of a generalised Planck law by investigation of the emission from GaAs luminescent diodes," *Journal of Physics: Condensed Matter,* vol. 2, no. 16, pp. 3803-3810, 1990.

[15] B. Ullrich, S. R. Munshi and G. J. Brown, "Photoluminescence analysis of p-doped GaAs using the Roosbroeck–Shockley relation," *Semiconductor Science and Technology,* vol. 22, no. 10, pp. 1174-1177, 2007.

[16] R. Bhattacharya, B. Pal and B. Bansal, "On conversion of luminescence into absorption and the van Roosbroeck-Shockley relation," *Applied Physics Letters,* vol. 100, no. 22, p. 222103, 2012.

[17] J. K. Katahara and H. W. Hillhouse, "Quasi-Fermi level splitting and sub-bandgap absorptivity from," *Journal of Applied Physics,* vol. 116, no. 17, p. 173504, 2014.

[18] A. Vaskuri, P. Kärhä, H. Baumgartner, O. Kantamaa, T. Pulli, T. Poikonen and E. Ikonen, "Relationships between junction temperature, electroluminescence spectrum and ageing of light-emitting diodes," *Metrologia,* vol. 55, no. 2, pp. S86-S95, 2018.

[19] G. P. Eppeldauer, C. C. Cooksey, H. W. Yoon, L. M. Hanssen, V. B. Podobedov, R. E. Vest, U. Arp, C. C. Miller and G. P. Eppeldauer, "Broadband Radiometric LED Measurements," in *Proc. SPIE Int. Soc. Opt. Eng.*, 2016.

[20] G. P. Eppeldauer, "Standardization of broadband UV measurements for 365 nm LED sources," *Journal of Research of the National Institute of Standards and Technology,* vol. 117, pp. 96-103, 2012.

[21] Bose, "Plancks Gesetz und Lichtquantenhypothese," *Zeitschrift für Physik,* pp. 178-181, 1924.

[22] L. Boltzmann, "Über die Beziehung zwischen dem zweiten Hauptsatze der mechanischen Wärmetheorie und der Wahrscheinlichkeitsrechnung, respective den Sätzen über das Wärmegleichgewicht," pp. 373-435, 1877.

[23] K. Sharp, "Translation of Ludwig Boltzmann's Paper "On the relationship between the second fundamental theorem of the mechanical theory of heat and probability calculations regarding the conditions for thermal equilibrium," *Entropy,* vol. 17, no. 4, pp. 1971-2009, 2015.

Creative engineering and manufacturing • Our engineering team is accustomed to developing products according to client's needs. In-house machining and assembling facilities shorten the time from concept to finished products.

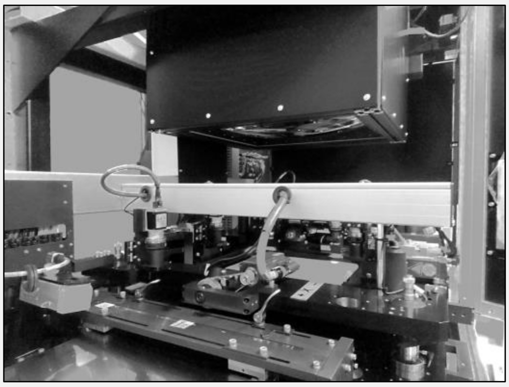

Customized UV-LED exposure system installed on a roll-to-roll machine

Visit our website to have an insight into our other products and activities. Contact us for further technical information and to obtain a quotation.

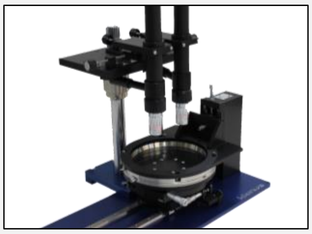

Double image microscope

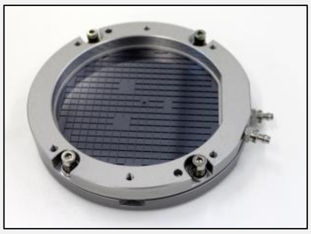

A model of wafer chuck

About idonus

Founded in 2004, idonus is a Swiss company that develops and manufactures special equipment for the MEMS and watchmaking industries. Our product portfolio includes UV-LED exposure systems for photolithography, IR microscope for wafer inspection, vapor phase chemical etcher for silicon-based devices. Since 2016, we also provide ion implantation services and machines for the surface treatment of materials.

Contact us for more details:

Christian Spoerl
Managing Director
sales@idonus.com

idonus

creative engineering and manufacturing

idonus sàrl
Rouges-Terres 61
CH – 2068 Hauterive

T: +41 32 724 44 40
info@idonus.com
idonus.com

© 2020 idonus sàrl. All rights reserved.